Preparation of Cellulose Whiskers Reinforced Nanocomposites from an Organic Medium Suspension

My Ahmed Saïd Azizi Samir,[†,‡] Fannie Alloin,[‡] Jean-Yves Sanchez,[‡] Nadia El Kissi,[§] and Alain Dufresne*[,⊥]

Centre de Recherches sur les Macromolécules Végétales (CERMAV-CNRS), Université Joseph Fourier, BP 53, F38041 Grenoble Cedex 9, France; Laboratoire d'Electrochimie et de Physico-chimie des Matériaux et des Interfaces (LEPMI-INPG), BP 75, F38402 St Martin d'Hères, France; Laboratoire de rhéologie (INPG), BP 95, F38402 St Martin d'Hères, France; and Ecole Française de Papeterie et des Industries Graphiques (EFPG-INPG), BP 65, F38402, St Martin d'Hères, France

Received October 20, 2003

ABSTRACT: The purpose of this study was to investigate a new way of processing cellulose whiskers reinforced polymer. A stable suspension of tunicin whiskers was obtained in an organic solvent (*N*,*N*-dimethylformamide) without a surfactant addition or a chemical surface modification. Both the high value of the dielectric constant of DMF and the medium wettability of tunicin whiskers were supposed to control the stability of the suspension. The nanocomposite materials were prepared by UV cross-linking using an unsaturated polyether as matrix. The resulting films were characterized by SEM, DSC, and mechanical testing in both the linear and nonlinear domains. The processing technique from a *N*,*N*-dimethylformamide suspension was found to be successful and led to materials whose properties are similar to those obtained with aqueous medium. It could be a good alternative to broaden the number of possible polymer matrices and to allow the processing of nanocomposite materials from an organic solvent solution instead of using aqueous suspensions.

Introduction

Polyoxyethylene (POE)-based polymers are the most commonly used materials for polymer electrolyte applications in lithium batteries due to their cationic solvatation ability. In a previous study,[1] it was shown that tunicin whiskers strongly increased mechanical properties of POE above its melting temperature without detrimental decrease of the ionic conductivity. However, from a practical point of view, the processing of a composite polymer electrolyte from an aqueous suspension of cellulose whiskers is not easy to consider since water can react with the negative electrode and reduce the battery cycle life.

Therefore, the main obstacle for the use of cellulose whiskers as a reinforcing phase in a wide variety of polymers is the limited stability of whiskers in aqueous suspension. To process nanocomposite materials with a good level of dispersion, the polymeric matrix must be either a hydrosoluble polymer or an aqueous suspension of polymer, i.e., a latex. Cellulose whiskers are very difficult to disperse in a polymeric matrix as they have a large surface area and possess large hydrogen forces among themselves. It can lead to the formation of strongly bound aggregates, as compared to polymer/clay nanocomposites, in which substituted cationic surfactants play a role in increasing hydrophobicity and in enhancing dispersion. A surfactant can be used to disperse cellulose whiskers in a nonpolar solvent.[2,3] Stable suspensions of cotton and tunicin whiskers in toluene were obtained by this way. However, the large amount of surfactant necessary to maintain the stability of the suspension, due to the high specific area of the filler, prevents the use of this technique for composites processing in organic solvents. The surface chemical modification of cellulose whiskers is another way to disperse cellulose whiskers in organic solvents. It generally involves reactive hydroxyl groups from the surface of whiskers.[4−6] However, the mechanical performances of the resulting composites were found to strongly decrease after chemical modification as reported for chitin whiskers from crab shell.[7] This loss of performance was supposed to be due to the partial or total destruction of the three-dimensional network of chitin whiskers assumed to be present in the unmodified composites.

In the present work, we show that it is possible to disperse tunicin whiskers in an organic solvent without either addition of a surfactant or any chemical modification. The birefringence and rheological behavior of this organic suspension were studied and compared to those of the aqueous suspension. Composites reinforced with tunicin whiskers were prepared in organic medium, and their thermal and mechanical properties were investigated.

Experimental Section

Tunicin Whiskers. Cellulose whiskers were extracted from tunicate (a sea animal). Colloidal suspensions of whiskers in water were prepared as largely described elsewhere.[8−10] Small fragments of external wall of tunicate that were deproteinized by three successive bleaching treatments and disintegrated in water with a Waring blender. The resulting aqueous tunicin suspension was mixed with sulfuric acid to reach a final acid/water concentration of 60 wt %. Hydrolysis was made at 65 °C for 30 min under strong stirring. The suspension was washed with water until neutrality was reached. The sulfate groups created during hydrolysis in the surface of whiskers are responsible of the good dispersion and stability of the aqueous suspension[10] after sonication in a Branson sonifier. After freeze-drying the suspension and drying for 48 h the

[†] CERMAV-CNRS.
[‡] LEPMI-INPG.
[§] Rhéologie-INPG.
[⊥] EFPG-INPG.
* To whom correspondence should be addressed: e-mail Alain.Dufresne@efpg.inpg.fr.

10.1021/ma030532a CCC: $27.50
Published on Web 01/20/2004

resulting powder at 100 °C under vacuum, the dried whiskers were stored in a glovebox. Suspensions of tunicin whiskers in *N*,*N*-dimethylformamide (DMF) were prepared by vigorously mixing dry whiskers until obtaining a homogeneous suspension. These suspensions were exposed to the high sonic vibrations to individualize whiskers in DMF. By this method, suspensions were prepared at different concentrations ranging from 0.5 to 2.4 wt %.

Matrix Synthesis. An unsaturated polyether was synthesized by reaction of a α,ω-dihydroxyoligopoly(oxyethylene) with a dihalide isobutenyl compound, 3-chloro-2-chloromethylpropene, according to the reaction reported by Alloin et al.[11,12] The PEG used in the present study was provided by Aldrich, and its molecular weight was 400 g mol^{-1}. The polymer obtained in aqueous solution after polycondensation was purified by ultrafiltration using a Filtron cell with a cutoff at 3000 g mol^{-1}. After purification, water was removed by freeze-drying. The resulting polymer labeled LPC400 (Linear PolyCondensate) was dissolved in DMF and stored in a glovebox. To prevent any degradation of the polymer, we protect the solution against light and thermal sources. Gel permeation chromatography (GPC) analysis was performed in tetrahydrofuran (THF) on a Waters 590 GPC instrument equipped with a differential refractometer Waters 410 and a Waters 745B data module. For calibration, polystyrene standard solutions were injected. The number-average molecular weight was $M_n = 2.64 \times 10^4$ g mol^{-1}.

Film Processing. Composites were prepared by UV radiation curing in argon atmosphere at room temperature. A homogeneous suspension was obtained by mixing the LPC400 solution and the suspension of whiskers in different compositions. A thermally stable photoinitiator, 4-(2-hydroxyethoxy)-phenyl-(2-hydroxy-2-propyl)ketone (HPPK) purchased from Ciba Specialty Chemicals, was added, and the suspension was cast into aluminum plates. The quantity of HPPK was fixed to 2% of reactive double bonds in LPC400. This low amount of photoinitiator was chosen to avoid high cross-linking density detrimental in battery applications. The solvent was allowed to slowly evaporate at 55 °C for 30 h in a glovebox. Cross-linking was carried out by using a mercury lamp at a distance of 10 cm with 10 min exposition time in a sealed apparatus in argon. Similar processing conditions were used to prepare the unfilled matrix. After cross-linking, the network was noted NPC400 (Network PolyCondensate).

Scanning Electron Microscopy (SEM). A JEOL JSM-6100 instrument was used for the investigation of composite morphology. The specimens were frozen under liquid nitrogen, then fractured, mounted, and coated with gold/palladium on a JEOL JFC-1100E ion sputter coater, and observed. SEM micrographs were obtained using 7 kV secondary electrons.

Rheological Behavior of Suspensions. Rheological data were collected with a rotating rheometer (Carrimed CSL2-100) operating under controlled torque (stress) conditions. The motor was mounted on air bearing, which reduces friction. Samples were tested using a cone/plate geometry with a diameter of 60 mm, a cone angle of 1°, and a gap of 24 μm. The setup worked in the frequency range 10^{-3}−40 Hz, with a maximum torque of 10 mN m, and angular displacement lower than 2.5 μrad can be measured.

A stress sweep test was conducted at 23 °C on each sample with stresses in the range from 30 to 0.5 Pa. The corresponding rotation speed was measured optically and allowed the shear rate to be calculated and thus determination of the flow curve. In the case of tests involving high rotation speeds, inertia effects were taken into account.

Heat Flow Microcalorimetry. The calorimetric measurements (Setaram-C 80 microcalorimeter) were performed in a two-compartment cell: a lower compartment, where 5 mg of whiskers was placed, and an upper compartment, where typically 500 mg of the different solvents was introduced. A PTFE membrane separated the two compartments. A reference cell of the same type was used, the upper compartment containing also 500 mg of the same solvent and the lower compartment being empty. The two cells were placed in the apparatus for temperature equilibration until the relative heat flow was below 50 μW. The PTFE membranes of the two cells were then pierced simultaneously by a movable steel needle. For all measurements, the temperature was fixed at 40 °C.

Differential Scanning Calorimetry (DSC). Differential scanning calorimetry (DSC) was performed using a DSC2920 CE modulated differential scanning calorimeter from TA. Around 15 mg of sample was placed in a pressure-tight DSC cell in glovebox. Each sample was heated from −100 to 110 °C at a heating rate of 10 °C min^{-1}. The glass transition temperature (T_g) was taken as the inflection point of the specific heat increment at the glass−rubber transition while the melting temperature (T_m) was taken as the peak temperature of the melting endotherm. The enthalpy of melting (ΔH_m) was calculated from the area of the melting endotherm.

Dynamic Mechanical Analysis (DMA). Dynamic mechanical tests were carried out with a spectrometer DMA Q800 from TA Instruments working in the tensile mode. The setup measured the complex tensile modulus E^*, i.e., the storage component E' and the loss component E'', as well as the ratio of the two components, i.e., tan δ ($= E''/E'$). Measurements were performed in isochronal conditions at 1 Hz in a nitrogen atmosphere, and the temperature was varied between −100 and 175 °C at a heating rate of 3 °C min^{-1}. The maximum strain ϵ was chosen around 5×10^{-4} so as to be in the domain of the linear viscoelasticity of the material.

Tensile Tests. The nonlinear mechanical behavior of composites and unfilled matrix was analyzed using an Instron 4301 testing machine in tensile mode, with a load cell of 100 N capacity. The specimens were thin rectangular strips (20 × 6 × 0.2 mm), and all the results were averaged over at least three specimens. The tests were performed at 25 °C and 55% relative humidity (RH) at a strain rate $d\epsilon/dt = 8.3 \times 10^{-4}$ s^{-1} (cross-head speed = 1 mm min^{-1}).

The true strain ϵ was determined by $\epsilon = \ln((L/L_0))$, where L and L_0 are the length of the specimen at the time of the test and the length at zero time, respectively. The true stress σ was calculated by $\sigma = F/S$, where F is the applied load and S is the cross-sectional area at the time of the test. Assuming that volume of the sample remained constant, $S = S_0(L/L_0)$, where S_0 is the cross-sectional area at zero time. From the stress−strain curves, the Young modulus (E) was determined from the slope of the low-strain region. The true stress at break σ_b and the ultimate elongation ϵ_b were also determined by $\sigma_b = F_b/S$, where F_b is the load at break and $\epsilon_b = \ln(1 + (\Delta L_b/L_0))$, where ΔL_b is the elongation at break.

Results and Discussion

Cellulose Whiskers Suspension in DMF. The constitutive cellulose fragments are parallelepiped rods with a length ranging from 500 nm up to 1−2 μm, and they are almost 15 nm in width. The average aspect ratio (nanometer scale diameter vs micrometer scale length) of these whiskers was estimated to be close to 70.[8] The birefringence of whiskers suspensions is largely used as a positive criterion for suspension stability.[13] This birefringence results from the sum of an intrinsic birefringence, related to the optical anisotropy of the cellulose ($\Delta n \approx 0.05$), and a flow birefringence induced by a shearing action carried out before observation.[14] The latter results from a macroscopic anisotropy due to the orientation of the whiskers. Figure 1 shows optical photographs of suspensions of tunicin whiskers observed in polarized light between crossed polars. The whiskers content was 0.5 wt % in both suspensions, and the suspending medium was either water (Figure 1a) or DMF (Figure 1b). In both cases, a strong birefringence is observed. This is an indication of the good level of dispersion of tunicin whiskers in DMF. The high value of the dielectric constant of DMF ($\epsilon = 36.7$ at 25 °C)[15] could explain the stability of the suspension. Indeed, the maintenance of disperse state of cellulose

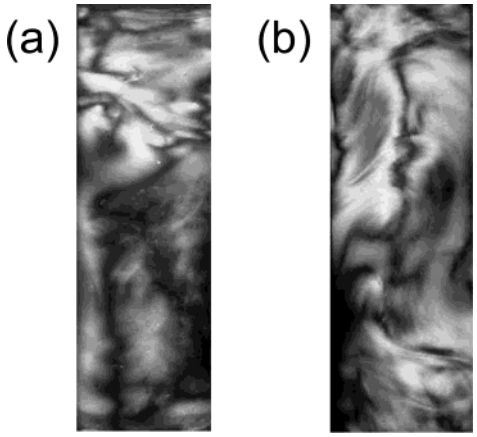

Figure 1. Photographs of suspensions of tunicin whiskers (0.5 wt %) in (a) water and (b) DMF observed between cross nicols, showing the formation of birefringent domains.

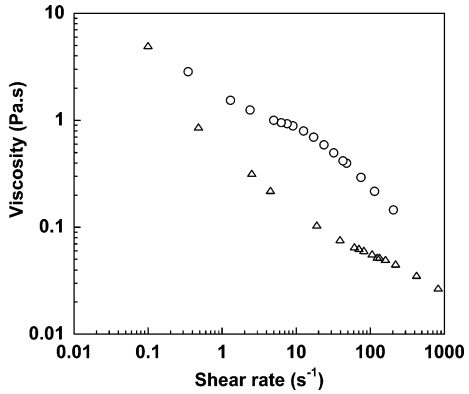

Figure 2. Viscosity vs shear rate for the suspensions of tunicin whiskers in DMF at concentration of (△) 1.2 and (○) 2.4 wt %.

whiskers requires the existence of an opposing interparticle repulsion[16] achieved in our case through electrostatic forces between charged whiskers.

Cellulose whiskers suspensions are interesting model systems to study the rheological behavior of rigid rodlike particles. Bercea and Navard[17] studied the shear dynamics of aqueous suspensions of tunicin whiskers. They show that whiskers can be easily oriented and the flow properties above a critical concentration are similar to thus of liquid crystal polymer solutions. Figure 2 displays the evolution of the whiskers suspension viscosity in DMF vs shear rate for two different concentrations. For the highest one (2.4 wt %), three well-defined regions are observed as reported by De Souza Lima[13] for aqueous suspensions of cotton linter. At low shear rate ($\dot{\gamma} < 1\ s^{-1}$), the viscosity is high and decreases monotonically with the shear rate. This shear thinning shows the alignment of whiskers under flow as observed by Orts et al.[18] and Ebeling et al.[19] in aqueous medium. At intermediate shear rate ($1-10\ s^{-1}$) the viscosity decrease is slighter. It is ascribed to a high level of order of cellulose whiskers due to interparticle interactions. These interactions could result in a high resistance to flow and explain this shear-rate-independent behavior. At higher shear rate ($\dot{\gamma} > 10\ s^{-1}$), this ordered structure breaks down and whiskers become individualized. This rheological behavior is typical of liquid crystalline polymers.[20]

At lower concentration of whiskers in DMF (1.2 wt %), a similar behavior is observed, but it shifts toward lower viscosities. In addition, the interparticle interactions are lower, resulting in a ill-defined intermediate plateau. Therefore, the rheological properties of tunicin whiskers in DMF are very similar to those reported for aqueous suspensions.

Table 1. Heat of Immersion (Δh_0), Liquid−Air Interfacial Tension (γ_{lv}), and Contact Angle (θ) Measured at 40 °C for Tunicin Whiskers with Water, DMF, and Dodecane

	water	DMF	dodecane
Δh_0 (J/g)	−52.25	−26.77	−1.15
(γ_{lv}) (J m^{-2})[a]	0.069	0.034	0.024
θ (deg)	24[b]	50	146

[a] Determined from ref 33 at 40 °C. [b] Contact angle value for water on tunicin whiskers film from ref 24.

Contact angle measurements were achieved in order to evaluate the affinity of different solvents for tunicin whiskers. Contact angles can be calculated indirectly by measuring the enthalpies of mixing of whiskers with solvents according to the theory developed by Adams et al.[21] and used by Yan et al.[22] to measure contact angles for fumed silica nanospheres with different solvents.

The heat of immersion, Δh_0 (J g^{-1}), was directly measured by mixing tunicin whiskers with water, DMF, and dodecane. Dodecane was used for comparison to display the behavior of hydrophilic cellulose whiskers in the presence of a highly hydrophobic solvent. Results are reported in Table 1. The enthalpies of mixing, h_i (J m^{-2}), were calculated according to the following equation:

$$h_i = \Delta h_0 / A_s \tag{1}$$

where A_s is the surface area per unit of mass of solids (around 170 m^2 g^{-1} for tunicin whiskers from geometric calculation).[23] The relationship between the contact angle (θ) and the enthalpy of mixing is given by

$$\cos(\theta) = \frac{-KT - h_i}{\gamma_{lv}} \tag{2}$$

where γ_{lv} is the liquid−air interfacial tension and K is the difference between the temperature dependence of solid−liquid interfacial tension, γ_{sl}, and that of solid surface tension, γ_s:

$$K = \frac{d\gamma_{sl}}{dT} - \frac{d\gamma_s}{dT} \tag{3}$$

For low-energy surfaces and if the solid−liquid interfacial tension can be assumed to be independent of temperature, then the value of K is 7×10^{-5} J m^{-2} K^{-1}.[24] Therefore, from the determination of the heat of immersion and interfacial tension γ_{lv} (values collected in Table 1),[15] the contact angles were evaluated. From these values and using eq 2, aberrant cos(θ) values were calculated. This discrepancy could originate from the assumed value of the surface area, which did not take into account the potential roughness of the cellulosic filler. Taking the cos(θ) value for water on a tunicin whiskers film surface reported from direct contact angle measurement ($\theta = 24°$),[25] we calculated the surface area of tunicin whiskers. We found $A_s = 615$ m^2 g^{-1}. This seems to display a rather large roughness of cellulose whiskers. This calculated A_s value was used for the determination of cos(θ) values for DMF and dodecane (Table 1). As expected, the contact angle is very high

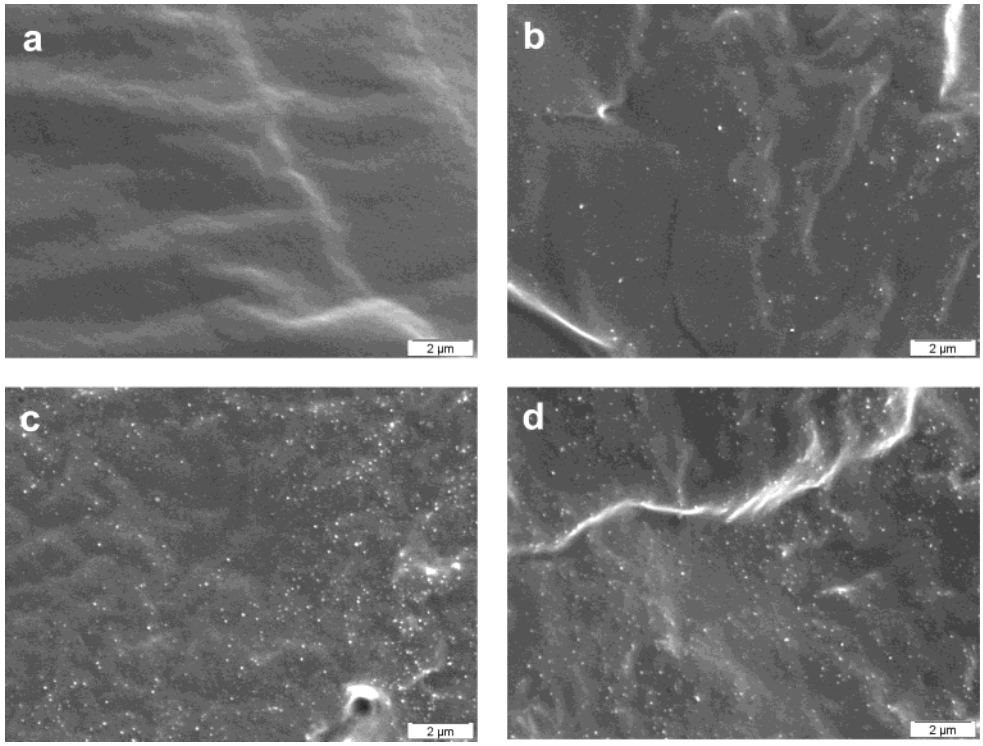

Figure 3. Scanning electron micrographs of the cryo-fractured surfaces of (a) unfilled NPC400 matrix and (b) 1, (c) 3, and (d) 6 wt % tunicin whiskers filled nanocomposite films.

with dodecane (θ = 146°), typical of the very poor affinity between the two components. This very high contact angle associated with the weak dielectric constant of dodecane (2 at 30 °C)[15] explains the total impossibility of dispersing cellulose whiskers in this solvent. The intermediate value calculated for DMF reflects the medium wettability of tunicin whiskers with this solvent. However, it seems that this wettability associated with a high dielectric constant is sufficient to disperse successfully cellulose whiskers in DMF.

Morphology of Nanocomposite Films. Solid polymer electrolyte, based on a lithium salt dissolved in a polymer matrix, often uses poly(oxyethylene) as matrix. Because of its high degree of crystallinity, a low ionic conductivity is obtained below the melting temperature. Several approaches have been suggested to improve the conducting properties. One of these is to use amorphous polymers. The polycondensate used in this study displays high performance as a polymer electrolyte.[11,26,27] Using LPC400 as linear polycondensate, amorphous network can be obtained.[11] A low amount of photoinitiator was chosen in the present study to avoid high cross-linking density that could reduce chain mobility and thus ionic mobility in the presence of lithium salt.

First, the efficiency of the cross-linking step of the nanocomposite films under UV was evaluated from the determination of the soluble part of the material. The weight loss (soluble fraction) of nanocomposite films when immersed overnight in acetonitrile was calculated from the difference in weight before and after immersion divided by the initial weight of matrix material. Acetonitrile was preferred to water to avoid any weight loss due to whiskers dispersion. The insoluble fraction was deduced, and values were corrected to account for the filler loading. Experimental data are collected in Table 2. It is observed that the insoluble fraction is systematically higher than 88 wt %. This is due to the high reactivity of the isobutenyl double bonds and to their random distribution along the polymeric chain. As the tunicin whiskers content increased, a monotonic increase of the soluble fraction of the matrix is reported. Therefore, the mean cross-linking density of the polymeric matrix decreases when the whiskers content increases. Because the cross-linking step was performed in situ in the presence of the omnipresent cellulose surface, this observation could be ascribed to an interfacial phenomenon. A possible explanation of the global decrease of the cross-linking density in composites is the presence of a weakly cross-linked region around the cellulosic filler particles (interphase), compared to the bulk cross-linking. Because of the high specific area of the tunicin whiskers, it could result in a global increase of the soluble fraction of matrix.

Table 2. Influence of Whiskers Content on Cross-Linking: Insoluble Fraction of Tunicin Whiskers Filled NPC400 Nanocomposites When Immersed in Acetonitrile

whiskers content (wt %)	insoluble fraction (wt %)
0	95
1	93
3	90
6	88

The examination of the cryo-fractured surface of tunicin whiskers filled nanocomposites prepared from a DMF solution was carried out using SEM. Parts a, b, c, and d of Figure 3 show the SEM of unfilled matrix and nanocomposite films filled with 1, 3, and 6 wt % tunicin whiskers, respectively. By comparing the micrographs showing the surface of fracture of unfilled matrix and of composites, it is easy to identify cellulose whiskers. In fact, tunicin whiskers appear like white dots. Their concentration is a direct function of the cellulose composition in the composite. These shinny dots correspond to the transversal sections of the cellulose whiskers. The fractured surface of the films is smooth, and the whiskers are highly individualized and

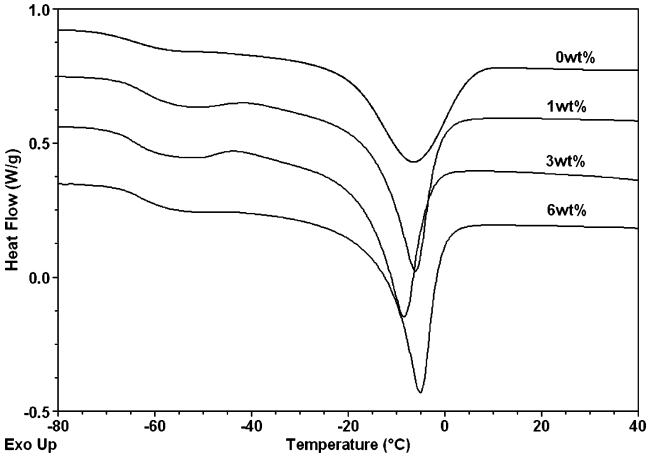

Figure 4. DSC thermograms of tunicin whiskers reinforced NPC400. The whiskers contents are indicated in the figure.

Table 3. Temperatures of the Calorimetric Transitions of Tunicin Whiskers Filled NPC400 Using Data Obtained from the DSC Curves: Glass−Rubber Transition Temperature (T_g), Melting Temperature (T_m) and Associated Heat of Fusion (ΔH_m), and Degree of Crystallinity (χ_c)

whiskers content (wt %)	T_g (°C)	ΔH_m (J/g)	T_m (°C)	χ_c[a]	T_α[b] (°C)
0	−65.0	34.2	−7.6	0.22	−51
1	−60.0	35.5	−6.2	0.22	−53
3	−63.2	34.3	−8.4	0.23	−58.4
6	−60.7	36.5	−5.0	0.23	−57.7

[a] $\chi = (\Delta H_m/\Delta H_m^0)(1/w)$, where w is the weight fraction of polymeric matrix material in the composite and ΔH_m^0 was calculated according to the following equation:[29] $\Delta H_m^0 = 178.6 + 0.629T_m - 283 \times 10^{-3}T_m^2$. [b] T_α represents the main relaxation temperature Associated with the maximum of tan δ peak obtained from DMA experiments.

homogeneously distributed within the matrix. No gradient of whiskers concentration within the sample thickness, as reported for wheat straw cellulose whiskers,[28] was observed. In conclusion, the SEM observations indicate the success of the processing of tunicin whiskers filled nanocomposite films from a DMF solution.

Thermal Behavior. DSC studies of unfilled and filled materials were performed. Figure 4 shows the DSC traces of NPC400 matrix and related nanocomposites reinforced with tunicin whiskers. In all the curves a specific heat increment was observed around −60 °C. It corresponds to the glass−rubber transition (T_g) of the polymeric matrix. The values of T_g are collected in Table 3.

In composites, the presence of whiskers can influence the values of T_g in two opposite ways. First, the solid surface of cellulose whiskers can induce a restricted mobility of polymer chains in the vicinity of the interfacial area (confinement of the polymer). It should result in a global shift of T_g toward higher temperatures. In an opposite way, a decrease of the cross-linking density of the polymeric matrix was observed in the presence of tunicin whiskers. This effect can result indirectly in a decrease of T_g. These two competitive effects could explain the weak variation of the values of T_g according to the whiskers content in composites.

In Figure 4 an endothermal peak arises around −5 °C. This transition is considered to be due to the melting of remaining crystalline NPC400 domains. This is an indication that despite the cross-linking step of the polymeric matrix, crystallinity still remains. It is most probably due to the low amount (2%) of photoinitiator used for the cross-linking step, which was not sufficient to prevent the crystallization of the matrix. Fully amorphous materials were obtained when a higher amount (10%) of photoinitiator was used (results not shown). The melting temperatures (T_m), the apparent enthalpies of fusion (ΔH_m), and degree of crystallinity (χ_c) are collected in Table 3. It is worth noting that the latter was calculated per gram of polymeric matrix in the composites. Therefore, the degree of crystallinity was obtained from the ratio of the apparent enthalpy of fusion of the sample and the heat of fusion of perfectly crystalline poly(ethylene oxide)[29] divided by the weight fraction of polymeric matrix material in the composite.

No significant variation of the melting point was reported. It ranges between −8.4 and −5.0 °C whatever the composition may be. This is an indication that the crystallites size of the NPC400 matrix is practically not influenced by the presence of the tunicin whiskers. The degree of crystallinity of the NPC400 matrix, around 22%, was also almost unaffected by the filler and practically composition-independent. These results were not obvious since the cellulosic nanocrystals were found to influence the cross-linking density of the matrix, which in turn could have an effect on its crystallization. In addition, in previous works a transcrystallization phenomenon was reported for tunicin whiskers reinforced poly(hydroxyoctanoate)[30] and waxy maize starch plasticized with glycerol.[25] These observations were ascribed to the possible anchoring effect of the filler, tunicin whiskers, acting as nucleating agents for the polymeric matrix. However, if present, these phenomena could be thwarted by the confinement of the polymer within the dense cellulosic network.

Dynamic Mechanical Analysis. Figure 5a shows the variation of the storage tensile modulus at 1 Hz as a function of temperature for unfilled NPC400 matrix together with tunicin whiskers reinforced composites. For low temperatures, it was difficult to observe any change in the modulus with variation in the filler loading. As it is well-known, the exact determination of the glassy modulus depends on the precise knowledge of the sample dimensions. In our case, the films were soft at room temperature, and it was very difficult to obtain a constant and precise thickness along these samples. To minimize this effect, the elastic tensile modulus, E', at −100 °C was normalized at 3.5 GPa for all the samples. This can be justified by the fact that the difference between the elastic modulus of the glassy polymer and lignocellulosic filler was not high enough to easily appreciate any change at the low filler loading used in the present study.

The curve corresponding to the unfilled matrix is typical of semicrystalline polymers. The storage modulus remains practically constant up to ∼−60 °C. At higher temperatures, a decrease in the elastic shear modulus was observed, corresponding to the glass−rubber transition. This modulus drop corresponds to energy dissipation displayed in a relaxation process where tan δ passes through a maximum (Figure 5b). This relaxation process, labeled α, involves the release of cooperative motions of long amorphous chain sequences. The rubbery modulus around 200 MPa is known to depend on the degree of crystallinity of the material. The crystalline regions act as physical crosslinks for the elastomer. In this physically cross-linked

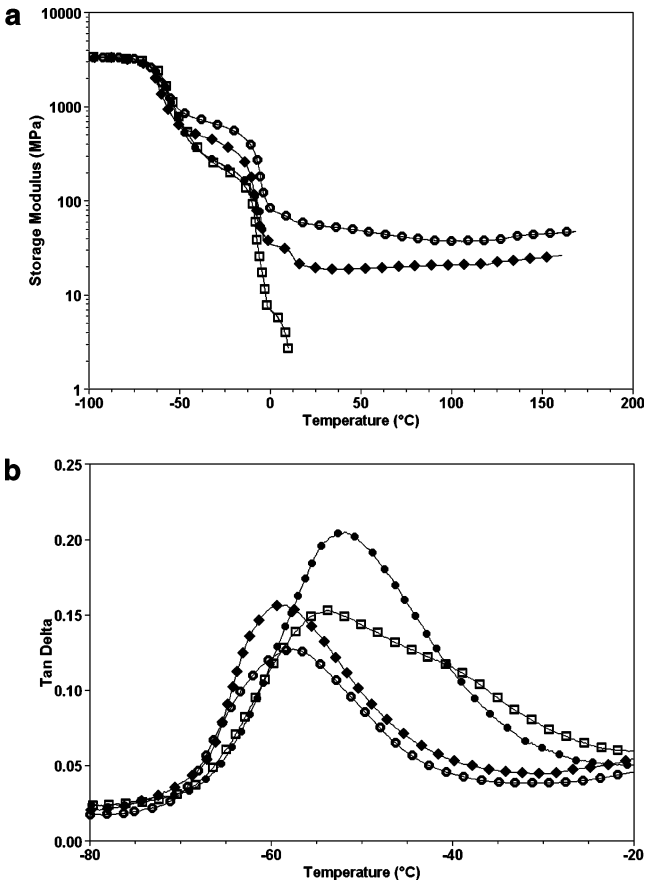

Figure 5. (a) Storage tensile modulus E' and (b) loss angle tangent tan δ vs temperature at 1 Hz for NPC400-based composites filled with (●) 0, (□) 1, (◆) 3, and (○) 6 wt % of tunicin whiskers.

system, the crystalline regions would also act as filler particles due to their finite size, which would increase the modulus substantially. In the terminal zone, corresponding to the melting of crystalline domains (∼−5 °C), the elastic tensile modulus drops sharply with temperature, and the experimental setup fails to measure it despite the chemical cross-linking of the material.

The dynamic mechanical behavior of the nanocomposite material filled with 1 wt % of tunicin whiskers is similar to the one of the unfilled matrix. This indicates that the mechanical behavior of the composite is matrix dominated for this filler loading level. At higher whiskers content, the differences are more significant. The rubbery modulus of the highly filled materials is substantially increased, and a thermal stabilization of the mechanical behavior can be observed above the melting point up to 170 °C. The rubbery modulus of the composite filled with 3 and 6 wt % of tunicin whiskers is around 500 and 900 MPa, respectively. As was observed before, the cross-linking density in composites decreased when the whiskers content increased, and the degree of crystallinity of the matrix was practically composition-independent. This indicates that the mechanical behavior of the material becomes whiskers dominated. Above 120 °C, a slight increase of the storage modulus is observed. It is most probably due the thermal cross-linking of the matrix.

Figure 5b shows the evolution of the mechanical loss factor tan δ as a function of temperature for NPC400 reinforced with tunicin whiskers in the low-temperature range. The temperature position, T_α, of the relaxation process associated with the anelastic manifestation of the glass−rubber transition of the amorphous domains of the polymeric matrix is listed in Table 3. T_α is directly linked to T_g of the matrix and to the drop of the storage tensile modulus (mechanical coupling effect). Because no significant variation of T_g was reported from DSC measurements with the whiskers content, the shift of T_α toward lower temperatures with increasing loading level is only ascribed to a mechanical coupling effect, which is more pronounced for highly filled samples. The magnitude of the tan δ peak, directly related to the modulus drop, depends on both the number of mobile entities and their contribution to the compliance. It decreases as the whiskers loading increases.

The strong difference in the storage modulus above T_g between 1 and 3 wt % of cellulose whiskers is not surprising since high mechanical properties of tunicin nanocrystals reinforced composites were ascribed to the formation of a rigid whiskers network within the host matrix.[8] The formation of this network was assumed to be governed by a percolation mechanism, and the percolation threshold was found to be 1 vol %, i.e., around 1.25 wt %, taking 1.5 and 1.2 g cm^{-3} for the density of crystalline cellulose and polymeric matrix, respectively.

After melting of the crystalline domains of the polymeric matrix around −5 °C, the mechanical stabilization around 25 and 60 MPa for the composites filled with 3 and 6 wt % of tunicin whiskers, respectively, is supposed to be mainly provided by the percolating cellulosic network. Previous studies[8,25,31,32] based on nanocomposites prepared from aqueous suspensions have shown that the high reinforcing effect of tunicin whiskers reinforced amorphous thermoplastic can be well predicted following the adaptation of the percolation concept to the classical phenomenological series-parallel model of Takayanagi et al.[33] The main advantage of this approach was to account for interactions between the fillers and for the hydrogen-bonding forces that hold the percolating cellulose whiskers network. Details of the calculation can be found elsewhere.[8,25,28,31,32] When the filler modulus is far higher than the one of the matrix, i.e., above T_m in our case, the predicted composite modulus, E_c, is simply given by $E_c = \psi E_R$,[32] where ψ and E_R correspond to the volume fraction and modulus of the stiff percolating network, respectively. It means that all the stiffness of the material results from infinite aggregates of tunicin whiskers.

It is of interest to compare the performances of nanocomposite materials prepared from DMF suspensions to the predicted data. The volume fraction ψ was calculated using the parameters already used in our previous studies: $v_{RC} = 1$ vol % for the percolation threshold and $b = 0.4$ for the critical exponent in a three-dimensional problem according to the percolation theory.[8,23,28,31,32] The tensile modulus, E_R, of a film of cellulose whiskers was measured from a tensile test performed on a film prepared by water evaporation of a tunicin whiskers suspension ($E_R = 8$ GPa). Literature reports values ranging between 5 and 15 GPa depending on the source of cellulose.[8,28,31] The calculated moduli are 35 and 106 MPa for the composites filled with 3 and 6 wt % of tunicin whiskers, respectively. These predicted data agree with the experimental data, which are around 25 and 70 MPa at room temperature, respectively. However, these experimental data could be affected by the low-temperature storage modulus nor-

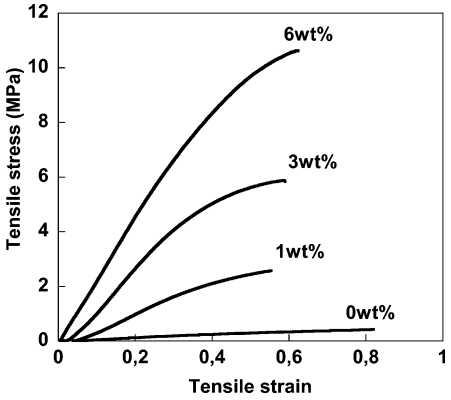

Figure 6. Typical true stress vs true strain curves of tunicin whiskers reinforced NPC400 (T = 25 °C, 55% RH, $d\epsilon/dt = 8.3 \times 10^{-4}$ s^{-1}). The tunicin whiskers contents are indicated in the figure.

Table 4. Mechanical Properties of Tunicin Whiskers Filled NPC400 Using Data Obtained from Tensile Tests: Tensile Modulus (E), Stress at Break (σ_b), and Elongation at Break (ϵ_b)

whiskers content (wt %)	E (MPa)	σ_b (MPa)	ϵ_b (%)
0	0.81	0.4	82
1	5.3	2.6	57
3	13.4	5.9	58
6	22.3	10.6	62

malization. This is a good indication that the preparation of nanocomposite materials reinforced with tunicin whiskers from a DMF suspension results in a good dispersion level of the filler, in agreement with SEM observations, and do no alter the formation of the percolating cellulosic network.

Tensile Tests. The nonlinear tensile mechanical behavior of the tunicin whiskers/NPC400 composite films was analyzed at room temperature. It is worth noting that at this temperature all samples were fully amorphous. Typical stress vs strain curves are shown in Figure 6. For each measurement, it was observed that the strain was macroscopically homogeneous and uniform along the sample, until its break. The lack of any necking phenomenon confirms the homogeneous nature of these composites at the scale of a few hundred nm^3. The samples exhibit an elastic nonlinear behavior typical of semicrystalline polymer at $T > T_m$. The stress continuously increases with the strain. The tensile modulus, tensile strength, and elongation at break of the films were determined from the plot of the stress vs strain as described in the Experimental Section. The results are collected in Table 4.

A clear increase of the Young modulus is observed by increasing the whiskers content. For instance, for a film containing only 6 wt % (~5 vol %) it is more than 27 times higher than that of the matrix. However, the modulus is systematically lower than the one measured from DMA experiments at room temperature (for the 3 and 6 wt % filled composites). This discrepancy could originate from the fact that dynamic mechanical measurements involve weak stresses. The possible interactions between percolating tunicin whiskers are not damaged under these weak stresses. Under the higher stress level, as applied in tensile tests, these interactions seem to be partially destroyed. In addition, the storage tensile modulus value can be affected by the low-temperature storage modulus normalization. In cross-linked polymers the modulus is assumed to be proportional to the cross-linking density. The molecular weight between cross-links (M_c) can be derived from the following equation:

$$M_c = \frac{3\rho RT}{E} \tag{4}$$

where ρ is the density of LPC400, R is the gas constant (8.32 J mol^{-1} K^{-1}), and T is the temperature in K. From the Young modulus value of the unfilled matrix, M_c was found to be around 9000 g mol^{-1}. The monomeric molecular weight of LPC400 being 454 g mol^{-1}, the average number of monomer units between cross-links is of the order of 20. The cross-linking efficiency is poor, and it seems that the radical propagation is difficult. This could be due to the steric entanglement, which favors transfer reactions. This poor cross-linking density is in accordance with the NPC400 semicrystalline behavior and the poor mechanical properties observed for the unfilled matrix. As the whiskers incorporation ensures the mechanical properties, this poor cross-linking efficiency is an advantage because high ionic conduction performance could be obtained in the presence of salt.

The stress at break also significantly increases with the whiskers content, whereas the elongation at break first decreases from 82% to 57% with the incorporation of 1 wt % of tunicin whiskers within the matrix and then remains roughly constant for higher loading level. It is therefore worth noting that the presence of tunicin whiskers in the polymeric matrix results in a significant increase of the modulus as reported above, without much lowering the elongation at break.

Conclusions

Nanocomposite materials reinforced with tunicin whiskers were successfully prepared from a *N*,*N*-dimethylformamide (DMF) suspension. The stability of this suspension was found to be as good as in water, owing the high value of the dielectric constant of DMF and medium wettability of tunicin whiskers. Composite materials were obtained via a DMF suspension that does not alter the formation of the percolating cellulosic network responsible for high mechanical properties. The SEM observations and mechanical performances indicate that the filler is well dispersed within the host matrix. The cross-linking density of the polymeric network was found to decrease with the whiskers content, most probably due to an interfacial effect. The presence of tunicin whiskers does not affect the thermal properties of the matrix. This investigation allows considering new applications for cellulose nanocrystals. Possible practical applications include the use of cellulose whiskers to reinforce composite polymer electrolytes for which water can react with the negative electrode and reduce the battery cycle life. Moreover, the use of DMF as the suspension medium allows some additional chemical modifications of whiskers. The processing and characterization of such composite materials were also investigated, and results will be published shortly.

Acknowledgment. The authors thank the Région Rhône-Alpes for financial support and Mrs. D. Dupeyre and M. M. Paillet for helping in SEM study and tunicin whiskers preparation, respectively.

References and Notes

(1) Alloin, F.; Azizi Samir, M. A. S.; Cavaillé, J. Y.; Dufresne, A.; Paillet, M.; Sanchez, J. Y. French Patent 0207746, 2002.
(2) Heux, L.; Chauve, G.; Bonnini, C. *Langmuir* **2000**, *16*, 8210.
(3) Bonnini, C.; Heux, L.; Cavaillé, J. Y.; Linder, P.; Dewhurst, C.; Terech, P. *Langmuir* **2002**, *18*, 3311.
(4) Gousse, C.; Chanzy, H.; Excoffier, G.; Soubeyrand, L.; Fleury, E. *Polymer* **2002**, *43*, 2645.
(5) Sassi, J. F.; Chanzy, H. *Cellulose* **1995**, *2*, 111.
(6) Araki, J.; Wada, M.; Kuga, S. *Langmuir* **2001**, *17*, 21.
(7) Gopalan Nair, K.; Dufresne, A.; Gandini, A.; Belgacem, M. N. *Biomacromolecules*, in press.
(8) Favier, V.; Cavaillé, J. Y.; Chanzy, H. *Macromolecules* **1995**, *28*, 6365.
(9) Wise, L. E.; Murphy, M.; d'Addiecco, A. A. *Pap. Trade J.* **1946**, *122*, 35.
(10) Marchessault, R. H.; Morehead, F. F.; Walter, N. M. *Nature (London)* **1959**, *184*, 632.
(11) Alloin, F.; Sanchez, J. Y.; Armand, M. *J. Electrochem. Soc.* **1994**, *141*, 1915.
(12) Alloin, F.; Sanchez, J. Y.; Armand, M. *J. Power Sources* **1995**, *54*, 34.
(13) De Souza Lima, M. Ph.D. Thesis, Bordeaux I, France, 2002.
(14) Van Krevelen, D. W. In *Properties of Polymers*; Elsevier: Amsterdam, 1990.
(15) Riddick, J. A.; Bunger, W. B. In *Techniques of Chemistry*, 3rd ed.; Wiley-Interscience: New York, 1970; Vol. 2.
(16) Russel, W. B.; Saville, D. A.; Schowalter, W. R. In *Colloidal Dispersions*; Cambridge Monographs on Mechanics and Applied Mathematics; Batchelor, G. K., Ed.; 1988.
(17) Bercea, M.; Navard, P. *Macromolecules* **2000**, *33*, 6011.
(18) Orts, W. J.; Godbout, L.; Marchessault, R. H.; Revol, J. F. In *Flow-Induced Structure in Polymers*; Nakatani, A. I., Dadmum, M. D., Eds.; ACS Symposium Series Vol. 597; Americain Chemical Society: Washington, DC, 1995; p 333.
(19) Ebeling, T.; Paillet, M.; Borsali, R.; Diat, O.; Dufresne, A.; Cavaillé, J. Y.; Chanzy, H. *Langmuir* **1999**, *15*, 6123.
(20) Onogi, S.; Asada, T. In *Rheology*; Astarita, G., Marrucci, G., Nicolais, L., Eds.; Plenum: New York, 1980; Vol. 3.
(21) Adams, A. W.; Liang, I. *Adv. Chem.* **1964**, *43*, 57.
(22) Yan, N.; Maham, Y.; Masliyah, J. H.; Gray, M. R.; Mather, A. E. *J. Colloid Interface Sci.* **2000**, *228*, 1.
(23) Dufresne, A. *Compos. Interfaces* **2000**, *7*, 53.
(24) Neumann, A. W. *Adv. Colloid Interface Sci.* **1974**, *4*, 105.
(25) Anglès, M. N.; Dufresne, A. *Macromolecules* **2000**, *33*, 8344.
(26) Sanchez, J. Y.; Alloin, F.; Benrabah, J.; Roux, C. *Macromol. Symp.* **1997**, *114*, 85.
(27) Ollivrin, X.; Farin, N.; Alloin, F.; Le Nest, J. F.; Sanchez, J. Y. *Electrochim. Acta* **1998**, *43*, 1257.
(28) Dufresne, A.; Cavaillé, J. Y.; Helbert, W. *Polym. Compos.* **1997**, *18*, 198.
(29) Domszy, R. C.; Mobbs, R. H.; Leung, Y. K.; Heatley, F.; Booth, C. *Polymer* **1979**, *20*, 1204.
(30) Dufresne, A.; Kellerhals, M. B.; Witholt, B. *Macromolecules* **1999**, *32*, 7396.
(31) Favier, V.; Canova, G. R.; Cavaillé, J. Y.; Chanzy, H.; Dufresne, A.; Gauthier, C. *Polym. Adv. Technol.* **1995**, *6*, 351.
(32) Dubief, D.; Samain, E.; Dufresne, A. *Macromolecules* **1999**, *32*, 5765.
(33) Takayanagi, M.; Uemura, S.; Minami, S. *J. Polym. Sci., Part C* **1964**, *5*, 113.

MA030532A